PRAMANA
— journal of
physics

© Indian Academy of Sciences

Vol. 58, Nos 5 & 6
May & June 2002
pp. 925–935

Study of the peak effect phenomenon in single crystals of 2H-$NbSe_2$

C V TOMY[1], D PAL[2], S S BANERJEE[2,3], S RAMAKRISHNAN[2], A K GROVER[2], S BHATTACHARYA[2,4], M J HIGGINS[4], G BALAKRISHNAN[5] and McK PAUL[5]

[1]Department of Physics, Indian Institute of Technology, Powai, Mumbai 400 076, India
[2]Tata Institute of Fundamental Research, Homi Bhabha Road, Mumbai 400 005, India
[3]Department of Condensed Matter Physics, Weizmann Institute of Science, 76100-Rehovot, Israel
[4]N.E.C. Research Institute, 4 Independence Way, Princeton, New Jersey 08540, USA
[5]Department of Physics, University of Warwick, Coventry CV4 7AL, UK
E-mail: grover@tifr.res.in

Abstract. The weakly pinned single crystals of the hexagonal 2H-$NbSe_2$ compound have emerged as prototypes for determining and characterizing the phase boundaries of the possible order–disorder transformations in the vortex matter. We present here a status report based on the ac and dc magnetization measurements of the peak effect phenomenon in three crystals of 2H-$NbSe_2$, in which the critical current densities vary over two orders of magnitude. We sketch the generic vortex phase diagram of a weakly pinned superconductor, which also utilizes theoretical proposals. We also establish the connection between the metastability effects and pinning.

Keywords. Peak effect; vortex phase diagram; order to disorder transformation; 2H-$NbSe_2$.

PACS Nos 74.25.Dw; 74.60.Ge

1. Introduction

Phase transformations in the flux line lattice (FLL) has been a subject of widespread interest for many years in high T_c as well as low T_c superconducting systems. In the mixed state of a type II superconductor, the changes in the spatial order of the FLL can be studied through the peak effect (PE) phenomenon, which is the occurrence of an anomalous maximum in the critical current density (J_c) while proceeding towards the upper critical field (H_{c2}) value. In weakly pinned superconductors, the PE is considered to arise as a consequence of the competition and interplay between the interaction amongst the vortex lines, which stabilizes the FLL, and the varieties of disorder (thermal fluctuations, quenched random inhomogeneities, etc.), which can limit the spatial and temporal region over which the vortex lines remain correlated. We present here a status report [1–9] of the detailed experimental studies (the ac susceptibility and the dc magnetization) of the vortex matter by probing the PE phenomenon in a weakly pinned, low T_c ($\sim$ 7 K) superconductor,

Table 1. Some characteristics of the weakly pinned single crystals of 2H-$NbSe_2$.

Sample	Transition temperature $T_c(0)$ (K)	Critical current density J_c (4.2 K, 1 T) (A/cm^2)	Resistance ratio $R_{300\ K}/R_{8\ K}$	Radial correlation length/ FLL constant R_c/a_0
A	7.22	$\sim$ 1–5	20	$\sim 10^2$
B	7.17	$\sim$ 50–100	16	$\sim$ 50
C	6.00	$\sim$ 1000	9	$\sim$ 10

2H-$NbSe_2$, with a layered structure. This compound can be prepared in the single crystal form with varying pinning strengths (see table 1). It is therefore possible to explore the competition and interplay between the interactions, thermal fluctuations and the pinning of the vortex matter. Actually, 2H-$NbSe_2$ has emerged to be an ideal system, a prototype, exemplifying the novel notions for both the static and the driven vortex matter. The samples studied here represent the three types of 2H-$NbSe_2$ crystals, with varying purity (and pinning strength) as given in table 1. Sample A is an extremely clean crystal with the weakest pinning [10,11] and the sharpest PE transition. Sample B is also a clean crystal that has the intermediate pinning strength. The typically weakly pinned crystal is the sample C, which has J_c values in the range of $\sim 10^3$ A/cm^2.

2. Results and discussion

2.1 *PE represents a sharp onset of disordering and depinning*

Figure 1 shows the real part of the ac susceptibility (χ') as a function of temperature for the purest crystal (sample A). For measuring χ', the samples were cooled in the nominal zero field before applying the dc magnetic field and recording the shielding response. The PE is easily recognizable in the isofield $\chi'(T)$ measurements ($H_{dc} = 4$ kOe in the present case). The χ' response is related to J_c through the Bean's critical state model relationship [12],

$$\chi' = -1 + \left(\frac{\alpha h_{ac}}{J_c}\right),$$

where h_{ac} is the amplitude of the ac field and α is a geometry and size dependent factor. This implies that the sudden enhancement of χ' response corresponds to an anomalous and rapid increase in J_c. The narrow temperature interval over which the PE occurs suggests that the PE marks the onset of a sudden transformation in the FLL. We can characterize four temperatures from an isofield scan of a kind shown in figure 1: T_{pl} – the onset temperature of the PE, T_p – the peak temperature of the PE, T_{irr} – the temperature above which the magnetization appears reversible under the given experimental conditions and $T_c(H)$ – the temperature at which the sample goes to the normal state (H_{pl}, H_p, H_{irr} and $H_{c2}(T)$, respectively can be marked out in the case of isothermal scans). The inset of figure 1 shows the expanded portion near the PE region. The anomaly occurring between T_{irr} and $T_c(H)$ represents the well-documented differential paramagnetic effect (DPE). The DPE usually signals the presence of a (nearly) pinning free state of the vortex matter. Note that the depinning commencing at the peak temperature T_p is extremely sharp, as the interval

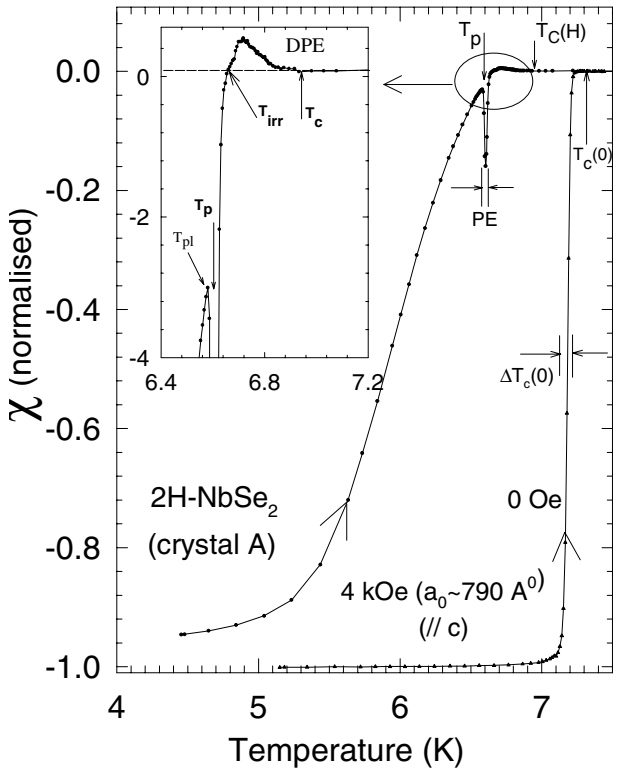

Figure 1. Temperature variation of the in-phase ac susceptibility (χ') data in the extremely weakly pinned crystal A of 2H-$NbSe_2$ for $H \| c$ [8]. The inset panel shows the identification of (i) the onset ($T_{\rm pl}$) and (ii) the peak positions of the peak effect, (iii) the irreversibility temperature ($T_{\rm irr}$) and the superconducting transition temperature ($T_{\rm c}$) in a field of 4 kOe. The paramagnetic response in $\chi'(T)$ sandwiched between $T_{\rm irr}$ and $T_{\rm c}$ identifies the differential paramagnetic effect (DPE). The superconducting transition width ($\Delta T_{\rm c}(0)$) in zero field and the region of the PE have also been marked for the comparison purpose.

($T_{\rm irr} - T_{\rm p}$) in figure 1 is smaller than the width of the superconducting transition in zero field.

2.2 *Disorder induced states of the FLL*

We present the influences of enhanced pinning and its relation to the thermomagnetic history effects on the PE in figure 2. The pinning strength is varied in two ways: (i) the conventional way of increasing the quenched random disorder in the samples during the preparation of the crystals (samples A, B and C) and (ii) by varying the applied external dc magnetic field. The measurements were performed for the two states of the FLL: the zero field-cooled (ZFC) and the field-cooled (FC) states. In the extremely weakly pinned states

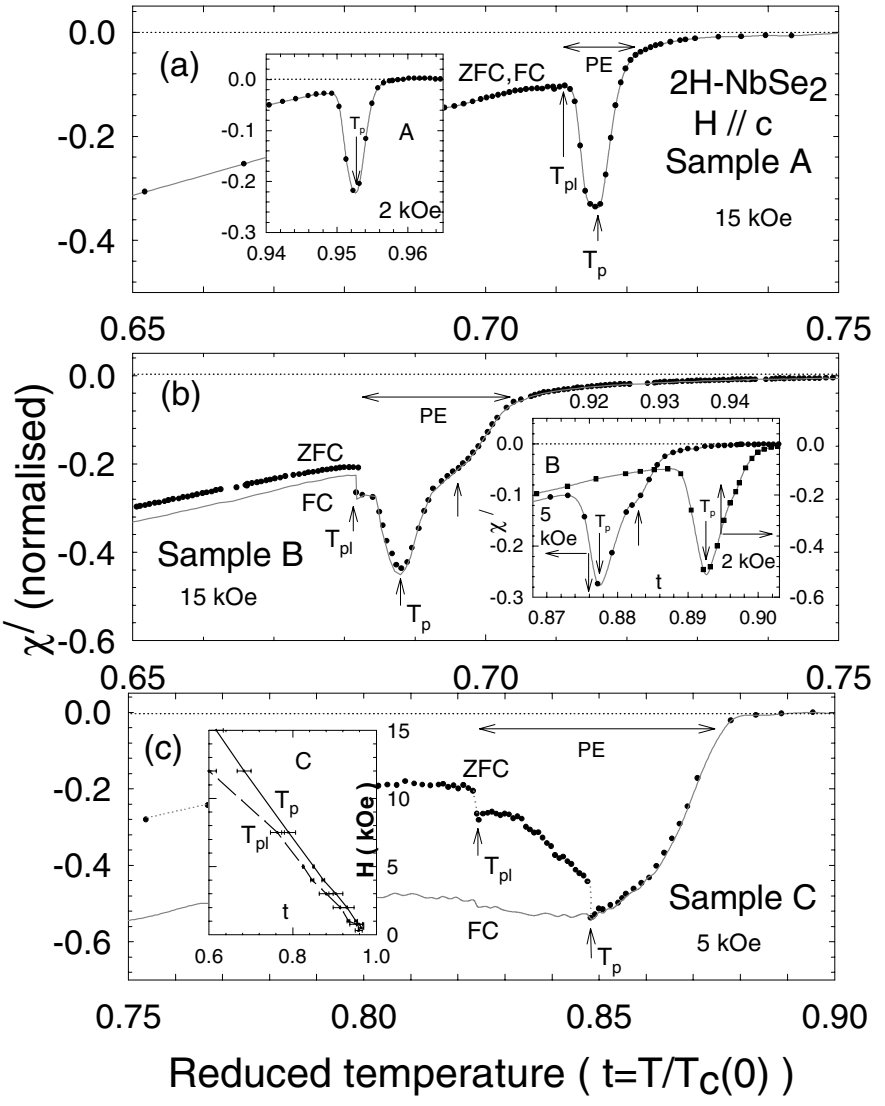

Figure 2. Isofield $\chi'(T)$ scans at the fields indicated in crystals A, B and C of 2H-$NbSe_2$ for the vortex states prepared in the zero field-cooled (ZFC) and the field-cooled (FC) manner [8]. In sample A, there is no difference in $\chi'(T)$ for the ZFC and the FC states up to 15 kOe. In sample B, the difference between $\chi'(T)$ responses for the ZFC and the FC states surfaces for $T < T_{\rm pl}$ above 10 kOe. In sample C, the difference between $\chi'(T)$ responses for the ZFC and the FC states can be seen for $T < T_{\rm p}$ even at 5 kOe. The inset panel in figure (c) shows the field variation of the onset and the peak temperatures of the PE, at which the abrupt dips in $\chi'(T)$ response occur in sample C.

(e.g. the sample A), the history effects are negligible and both the ZFC and FC curves follow the same path (figure 2a). As the pinning strength increases (from sample A to sample B as shown in figure 2b), the thermomagnetic history effects start to appear. Even though the ZFC and FC curves follow the same path at lower fields (inset of figure 2b), they start to differ at higher fields ($H_{dc} = 15$ kOe in the main panel of figure 2b) and the PE region starts broadening. In the ZFC curve, a sharp jump occurs at T_{pl}, which is absent in the cleanest sample A. As the pinning is further increased (cf. sample C and figure 2c), the thermomagnetic history effects increase and the PE region becomes very broad. The ZFC curve shows an additional sharp jump at T_p, also. Both the sharp transitions located at T_{pl} and T_p are less than 1 mK in width, and they signify the first order like transitions in the vortex state. In all the cases, the difference between the ZFC and the FC responses disappear above T_p, where the memory effects cease. Thus, we see that for the same field value (e.g., 15 kOe), the thermomagnetic history effects increase significantly, as we increase the pinning strength. Similarly, the increase in the history effects in the same sample as the field is increased demonstrates that increasing H results in observations equivalent to those evident via increasing the quenched disorder (pinning strength) at the same field. This in turn, indicates that the jumps observed at T_{pl} and T_p are disorder induced. It can easily be shown that the disorder-induced transition at T_{pl} corresponds to a *fracturing* of the FLL from a more ordered (nearly dislocation free) lattice to a highly amorphous vortex lattice. This could find an analogy with the transition predicted by Giamarchi and Le Doussal [13] from a Bragg glass state (free of dislocations) to a vortex (plastic) glass state, in which the dislocations proliferate. The jump at T_p further marks a transition from this partially amorphized vortex state into a completely amorphous state.

2.3 *Effect of thermal cyclings across the PE region*

A further evidence for the fracturing of the FLL and the existence of a novel open hysteresis loop within the PE region can be obtained through the thermal cycling studies [2] in the PE region as shown in figure 3. The FLL is zero-field cooled to the lowest temperature and is warmed up to a pre-selected temperature T such that (i) $T < T_{pl}$, (ii) $T_{pl} < T < T_p$ and (iii) $T > T_p$. When $T < T_{pl}$, i.e., at temperatures below the onset of the PE, the cool-down cycle retraces (filled diamonds) the ZFC curve (dashed line in figure 3). For $T > T_p$, χ' curve initially retraces the ZFC curve (filled inverted triangles), but below T_p, it crosses over to a FC- like state, instead of following the more ordered ZFC state. This indicates that the states above T_p are completely amorphous and history independent and these disordered states can be supercooled below T_p. However, if the sample is cooled from a temperature in the PE region ($T_{pl} < T < T_p$), it first tries to retrace the ZFC curve (see the open circles in the figure), overshoots it, and eventually drops sharply to the more disordered FC state. In the PE region (i.e., $T_{pl} < T < T_p$), the FLL is supposed to be in a fractured state. Upon lowering the temperature from such a state, the lattice stiffens, stresses build up and the system fails to drive out the dislocations in order to heal back to the ZFC state. Instead, it fractures further in order to relieve the stresses and hence, reaches the more disordered FC state. Such a behavior can constitute an open hysteresis in T, i.e., one cannot recover the original ZFC state by cycling in T alone. Any attempt to get the vortex matter out of the PE region by thermal cycling invariably leads to the more disordered FC state.

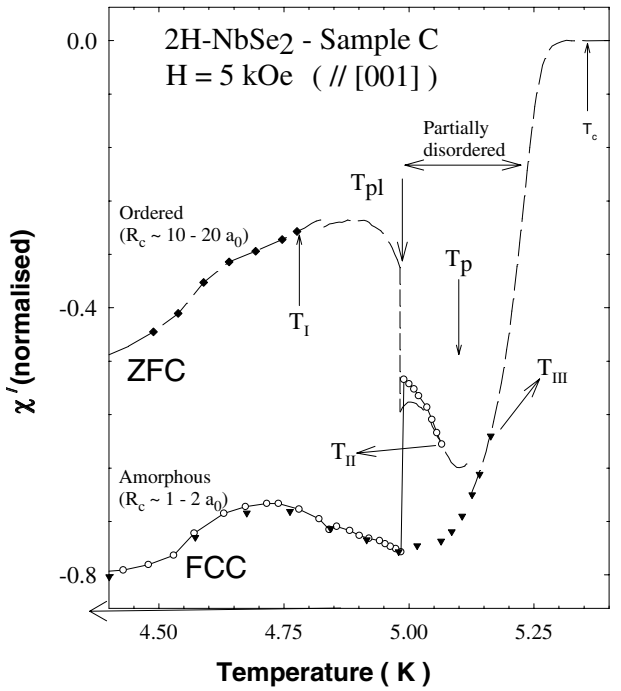

Figure 3. Display of $\chi'(T)$ response at 5 kOe ($H \| c$) in sample C as the temperature is lowered from $T_{\rm I}$ ($< T_{\rm pl}$), $T_{\rm II}$ ($T_{\rm pl} < T < T_{\rm p}$) and $T_{\rm III}$ ($T > T_{\rm p}$) [8]. The dashed curve denotes the $\chi'(T)$ response for the vortex state initially prepared at 5 kOe in the ZFC manner.

2.4 *Re-entrant behavior of the anomaly in* $J_{\rm c}(H,\ T)$

We have earlier shown [1] that the loci of the peak temperatures of the PE phenomenon are re-entrant through ac susceptibility measurements, for both the orientations of the sample B ($H \parallel c$ and $H \perp ab$). In figure 4, we display the re-entrant behavior of the PE via dc transport measurements. The inset of the figure shows that the PE manifests itself as a dip in $R(T)$. The shape of the PE curve in the main panel clearly demonstrates the re-entrant behavior, with a turnaround occurring at about 180 Oe. This re-entrant characteristic of the PE imparts a nose-type shape for the $T_{\rm p}(H)$ line in the H–T phase diagram, as shown in the inset panel (b) of figure 4. In addition to the ac susceptibility and dc resistance measurements, our dc magnetization measurements also clearly reveal the existence of the re-entrant nature of the anomaly in $J_{\rm c}(H,\ T)$ behavior [4].

2.5 *Vortex phase diagram*

Collating all the data from various measurements, we can construct a generic phase diagram for a weakly pinned type II superconductor, as shown in figure 5. The $H_{\rm pl}(T)$ line

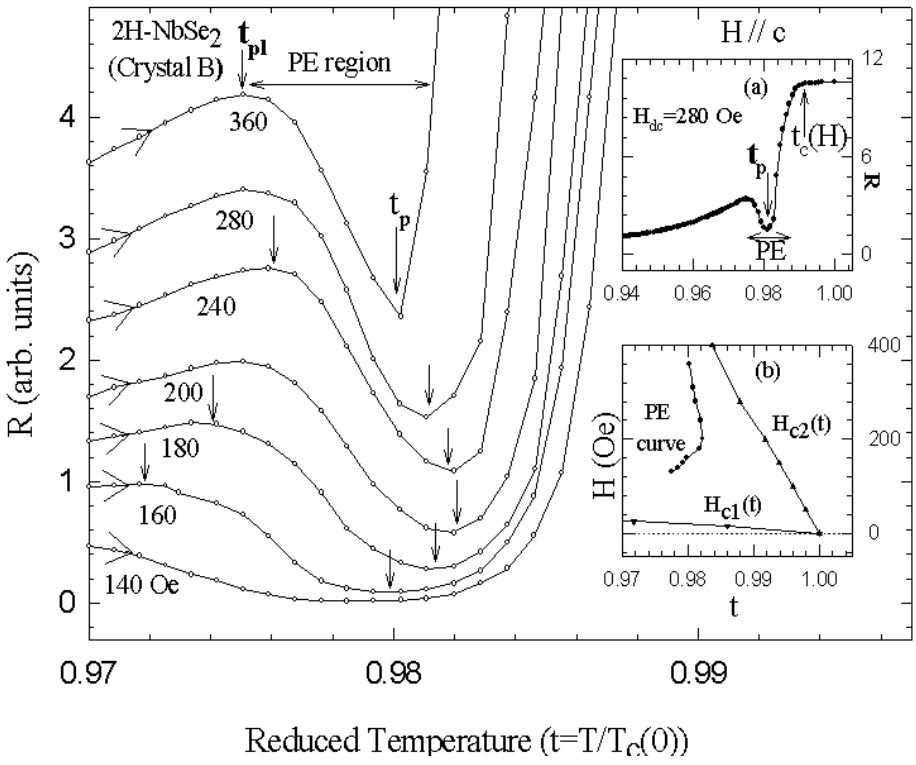

Figure 4. Temperature variation of the dc electrical resistance R across the PE region in sample B at the fields indicated ($H \| c$) [8]. The upper inset shows the $R(T)$ behavior in $H = 280$ Oe over an extended temperature interval to facilitate the identification of the PE phenomenon. The lower inset displays the temperature variation of (reduced) peak temperatures as determined from the $R(t)$ plots. The 'nose feature' in the PE curve passing through the $t_p(H)$ values is evident.

corresponds to the fracturing transition at the onset of the PE, T_{pl}. The $H_p(T)$ line corresponds to the peak positions of the PE, which marks the boundary for the transition to the completely amorphized vortex state, where the thermomagnetic history effects cease to exist. The $H_{irr}(T)$ line mark the quasi-reversible regime of the vortex matter (characterized by the DPE). Even though the $H_p(T)$ (or $T_p(H)$) line marks the transition to the amorphous state, the reversible behavior starts only after the $H_{irr}(T)$ (or $T_{irr}(H)$) line. Hence, the region between $H_p(T)$ and $H_{irr}(T)$ behaves as the pinned amorphous state and the region above $H_{irr}(T)$ (but less than H_{c2}) becomes the unpinned amorphous state. The various other phases are also marked in the phase diagram. An additional new line added to the usual vortex phase diagram is the re-entrant disorder line at low fields and close to T_c. This feature is due to the ordered vortex matter getting sandwiched between the disordered phases of the vortex matter at low and high fields. Detailed investigations of this re-entrant behavior as a function of the pinning strength (the inset of figure 5) have clearly demonstrated that the re-entrant disordered phase seen in our experiments is more close

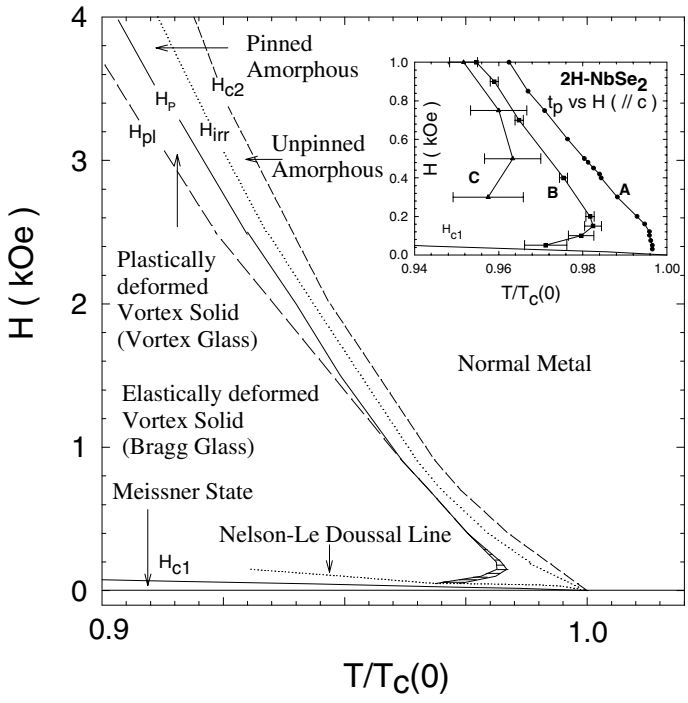

Figure 5. A schematic view of the vortex phase diagram at low fields and high temperatures (close to $T_c(0)$) in weakly pinned single crystals of 2H-$NbSe_2$ for $H \| c$ [5]. The inset shows the plot of (reduced) peak temperatures $t_p(H)$, in crystals A, B and C of 2H-$NbSe_2$ for $H \| c$.

to the theoretically predicted re-entrant glass phase than the re-entrant molten phase of a pinning-free, well ordered vortex solid.

2.6 *PE as a dynamical transition*

The results described so far support the notion that the peak position of the PE marks a sudden, i.e., the first-order-like transition for the vortex lattice. However, some recent results give the indication that the PE may be a dynamical transition. For instance, a few characteristics depend on the sweep rate of the magnetic field and the ac frequency. Figure 6 gives the shift of the peak position of the PE as a function of the sweep rate of the magnetic field. The inset on the right hand side of figure 6 shows a typical isofield scan (measurements were performed on a VSM), where the magnetization is shown against the applied field. The anomaly in the magnetization corresponds to the PE, with H_p marking the peak position of the PE. The expanded version of the PE region in sample A is shown in the left inset, where the magnetization is plotted for two sweep rates of the magnetic field. It is quite evident that the peak position, H_p, shifts as a function of the sweep rate and the hysteresis width decreases as the sweep rate is decreased from 80 to 8 Oe/s. An

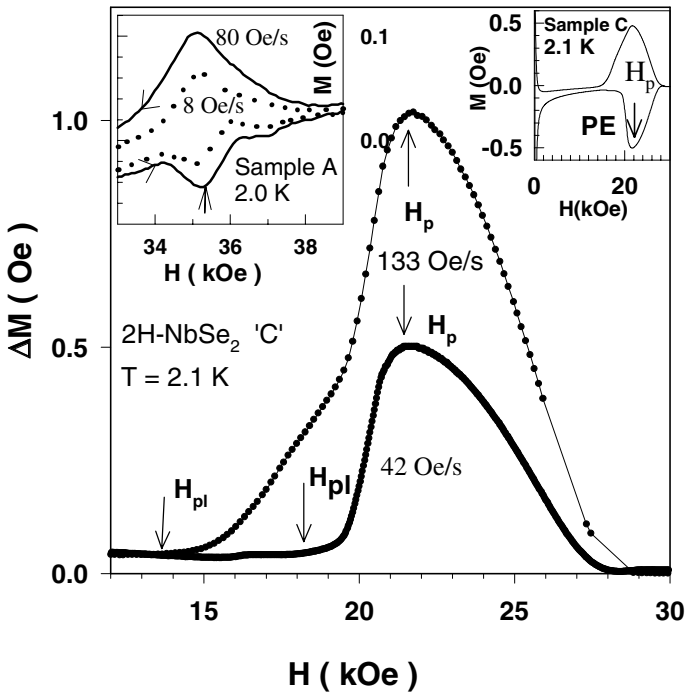

Figure 6. The inset on the top-right shows the identification of the PE anomaly in the M–H loop obtained using a vibrating sample magnetometer (VSM) in crystal C of 2H-$NbSe_2$ at 2.1 K. The inset panel on the top-left shows the PE bubbles in crystal A at 2 K, obtained using two different sweep rates for the dc magnetic field. The main panel of the figure shows the plot of the hysteresis widths ($\propto J_c(H)$) vs. field in sample C at 2.1 K, for the two different sweep rates of the dc field [9].

important observation here is the survival of the hysteresis till H_{c2}, which implies that H_{irr} is absent in this particular measurement, where the time scale is rather short ($\sim 10^{-2}$ s). This in turn suggests that H_{irr} line in the vortex phase diagram in figure 5 may not represent a sharp phase boundary. In the main panel of figure 6, we have plotted ΔM as a function of H in sample B. It clearly demonstrates the changes in the characteristics of the PE for different sweep rates; H_p decreases, while the onset field of the PE, H_{pl} enhances with the decrease of the sweep rate. The shift in the peak position of the PE as a function of frequency in the ac susceptibility measurements performed on sample A is depicted in figure 7 for an isofield, and in figure 8 for an isothermal measurement. The frequency dependence measurements were performed using a quantum design SQUID magnetometer. It is apparent that the boundary marking the peak position of the PE would shift upwards as the frequency is increased, thereby providing evidence for the dynamical nature of the PE.

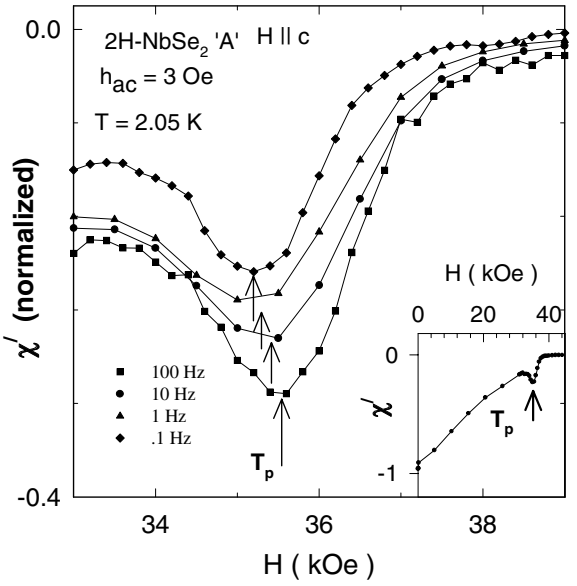

Figure 7. Portions of the isothermal $\chi'(T)$ plots at 2 K in crystal A of 2H-$NbSe_2$ for different frequencies. The inset shows the $\chi'(H)$ plot at 100 Hz over the entire field range [9].

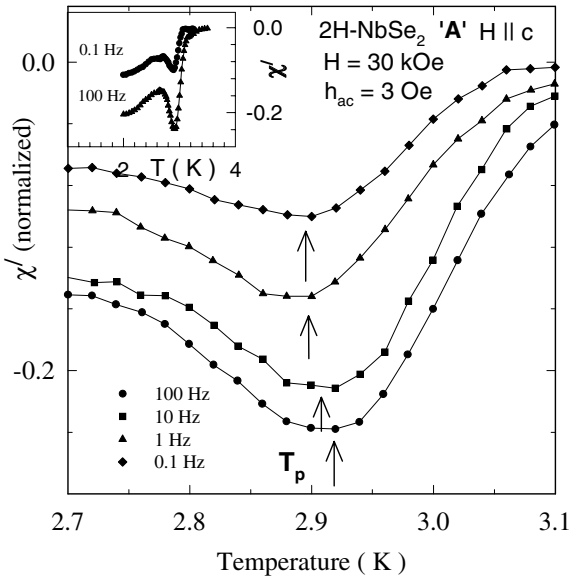

Figure 8. Portions of the isofield ($H = 30$ kOe) $\chi'(T)$ plots in crystal A of 2H-$NbSe_2$ at different frequencies. The inset shows the $\chi'(T)$ curves at 0.1 Hz and 100 Hz over the entire temperature range [9].

3. Summary

To summarize, we have provided a glimpse into a variety of experimental results pertaining to the peak effect in weakly pinned single crystals of 2H-$NbSe_2$. These results tend to support the notion of the peak effect as representing an occurrence of a transformation in the well-ordered state of the vortex matter over a narrow field/temperature interval. Noteworthy changes happen in the metastability and memory behavior between the onset and the peak positions of the peak effect. These results also establish a connection between the metastability and the (effective) pinning. However, the precise values of the field/temperature marking the change in the state of order of the vortex lattice appear to depend on the time scale of the experimental measurements.

Acknowledgements

One of us (DP) would like to thank the TIFR endowment fund for the partial financial support in the form of the Kanwal Rekhi Career Development Award.

References

[1] K Ghosh *et al*, *Phys. Rev. Lett.* **76**, 4600 (1996)
S S Banerjee *et al*, *Physica* **B237–238**, 315 (1997)
[2] S S Banerjee *et al*, *Phys. Rev.* **B58**, 995 (1998)
[3] S S Banerjee *et al*, *Phys. Rev.* **B59**, 6043 (1999)
[4] S S Banerjee *et al*, *Phys. Rev.* **B62**, 6699 (2000)
[5] S S Banerjee *et al*, *Physica* **C308**, 25 (1998)
[6] S S Banerjee *et al*, *Europhys. Lett.* **44**, 91 (1998)
[7] D Pal *et al*, *Physica C* (to be published)
[8] S S Banerjee, Ph.D Thesis (University of Mumbai, 2001)
[9] D Pal, Ph.D Thesis (University of Mumbai, 2002)
[10] M J Higgins and S Bhattacharya, *Physica* **C257**, 232 (1996)
[11] P H Kes *et al*, *Nature* **376**, 729 (1995)
[12] X S Ling and J I Budnick, in *Magnetic susceptibility of superconductors and other spin systems* edited by R A Hein, T L Francavilla and D H Leibenberg (Plenum Press, New York, 1991) p. 377
[13] T Giamarchi and P Le Doussal, *Phys. Rev. Lett.* **72**, 1530 (1994); *Phys. Rev.* **B52**, 1242 (1995)